A Three Revolute-Revolute-Spherical wearable fingertip cutaneous device for stiffness rendering

Francesco Chinello, Claudio Pacchierotti, Monica Malvezzi, Domenico Prattichizzo

A Three Revolute-Revolute-Spherical wearable fingertip cutaneous device for stiffness rendering

Francesco Chinello, Claudio Pacchierotti, Monica Malvezzi, and Domenico Prattichizzo

Abstract—We present a novel three Revolute-Revolute-Spherical (3RRS) wearable fingertip device for the rendering of stiffness information. It is composed of a static upper body and a mobile end-effector. The upper body is located on the nail side of the finger, supporting three small servo motors, and the mobile end-effector is in contact with the finger pulp. The two parts are connected by three articulated legs, actuated by the motors. The end-effector can move toward the user's fingertip and rotate it to simulate contacts with arbitrarily-oriented surfaces. Moreover, a vibrotactile motor placed below the end-effector conveys vibrations to the fingertip. The proposed device weights 25 g for 35×50×48 mm dimensions. To test the effectiveness of our wearable haptic device and its level of wearability, we carried out two experiments, enrolling thirty human subjects in total. The first experiment tested the capability of our device in differentiating stiffness information, while the second one focused on evaluating its applicability in an immersive virtual reality scenario. Results showed the effectiveness of the proposed wearable solution, with a JND for stiffness of 208.5 ± 17.2 N/m. Moreover, all subjects preferred the virtual interaction experience when provided with wearable cutaneous feedback, even if results also showed that subjects found our device still a bit difficult to use.

Index Terms—Haptic interfaces, wearable haptics, cutaneous devices, fingertip devices, softness rendering

1 Introduction

Wearable haptics is recently gaining great attention in the haptics and robotics fields. The demand for lightweight, compact, and unobtrusive wearable interfaces challenges researchers to pursue innovative solutions to make existing technologies more portable and wearable. Commercially-available wearable devices, such as the Apple Watch, the Motorola Moto 360, and the Microsoft Band, already provide simple vibrotactile haptic feedback to the wearer. For example, the Apple Watch embeds a linear actuator that can make the watch vibrate. It is used whenever the wearer receives an alert or notification, or to communicate with other Apple Watch owners. There are also applications being specifically developed to exploit the haptic capabilities of these devices. For example, the application "Feel The Wear", available in the Google PlayStore, enables the user to create custom vibration patterns by simply tapping the screen; and the application "Touch Room", available in the Apple's AppStore, enables two users that are far away to feel each other's touch through the screen of the device.

However, although quite interesting and promising, the haptic stimuli provided by these devices are still limited to vibrations, reducing the possibility of simulating rich contact sensations. Toward more compelling interactions, researchers have recently focused on wearable fingertip devices providing tactile stimuli through moving tactors, which are able to translate, rotate, and orient to simulate haptic interaction with different surfaces. Frisoli et al. [1] presented already in 2008 a fingertip haptic display for improving curvature discrimination using a moving platform. The device is designed to bring a plate into contact with the fingertip at different orientations, defined by the normal to the virtual surface at the point of contact. The system is composed of a parallel platform, actuating a translation stage for positioning the plate relatively to the fingerpad, and of a serial wrist, in charge of adjusting its orientation. The device is actuated via sheathed tendons. A more portable and improved design solution of the same concept has been later developed in [2], [3]. A voice-coil actuator was introduced for simulating fast contact transition, and the overall system mobility was reduced to 3-degrees-of-freedom (3-DoF): two degrees of freedom for the orientation and one linear degree of freedom to control the contact force at the fingertip. Gabardi et al. [4] further improved the above design by replacing sheathed tendons actuation with DC motors mounted directly on the joints. Moreover, they increased the portability and wearability of the system by reducing the overall weight and dimensions. The total weight of this device is now only 30 g for $66 \times 35 \times 38$ mm dimensions.

Similarly, Prattichizzo et al. [5] presented a wearable 3-degrees-of-freedom (3-DoF) cutaneous device for the fingertip. It consists of two platforms: one is located on the back of the finger, supporting three small DC motors, and the other one is in contact with the volar surface of the fingertip. The motors shorten and lengthen three cables to move the platform toward the user's fingertip and re-angle it to simulate contacts with arbitrarily oriented surfaces. Tsetserukou et al. [6] developed a 2-DoF wearable fingertip cutaneous device. It is composed of two DC motors driving a five-bar linkage mechanism mounted at the sides of the fingertip. Similarly to [7], when motors rotate in the same direction the linkage slides tangentially on the finger pad. On the other hand, when motors rotate in the same direction, the linkage moves towards or away from the fingertip. More recently, Leonardis et al. [8] presented a 3RSR wearable skin stretch cutaneous device

- *F. Chinello is with the Dept. of Business Development and Technology at Aarhus University in Herning, Midtjylland, Denmark. E-mail: chinello@btech.au.dk*
- *C. Pacchierotti is with the CNRS at Irisa and Inria Rennes Bretagne Atlantique, Rennes, France. E-mail: claudio.pacchierotti@irisa.fr.*
- *M. Malvezzi and D. Prattichizzo are with the Dept. of Information Engineering and Mathematics, University of Siena, Siena, Italy and with the Dept. of Advanced Robotics, Istituto Italiano di Tecnologia, Genova, Italy. E-mail: {malvezzi, prattichizzo}@diism.unisi.it.*

- *This research has received funding from the European Union Seventh Framework Programme FP7/2007-2013 under grant n°601165 of the project "WEARHAP - WEARable HAPtics for humans and robots," and from Rennes Métropole under the "Allocation d'Installation Scientifique (AIS) 2017" programme.*

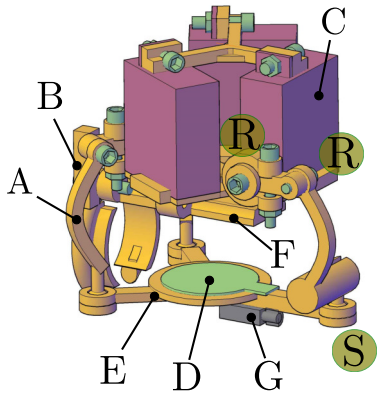

(a) CAD sketch.

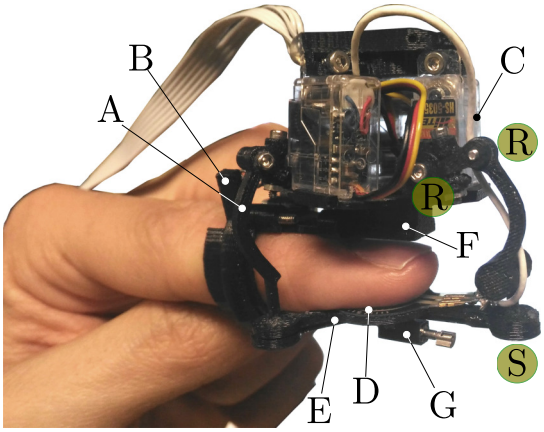

(b) Prototype.

Fig. 1: The proposed 3-DoF fingertip cutaneous device. It is composed of a static upper body (F) and a mobile platform (E): the body is located above the nail, supporting three servo motors (C), while the mobile platform contacts the finger pulp. Three legs (A) connect the mobile platform with the static body. Each leg is composed of two rigid links connected to each other and then with the body and the mobile platform, according to a RRS (Revolute-Revolute-Spherical) kinematic chain. The three upper revolute joints are actuated by the servo motors, and a piezoresistive sensor (D) measures the force applied by the mobile platform to the fingertip. A vibrotactile motor (G), attached below the platform, provides additional vibrotactile stimuli to the wearer. Finally, a clamp (B) enables the user to easily wear the device on the finger.

for the fingertip. An asymmetrical 3RSR configuration allowed compact dimensions with minimum encumbrance of the hand workspace and minimum inter-finger interference. Girard et al. [9] developed a wearable haptic device able to simulate 2-DoF shear forces at the fingertip. It is composed of a parallelogram structure actuated by two DC motors able to move a peg responsible for the shear feedback. It weights only 22 g for a total dimension of 20×34×35 mm.

The above mentioned devices have been used for the rendering of shapes, forces, and compliance. In the last couple of years, the rendering of softness/compliance have became a popular topic in haptics research. Softness represents indeed one of the most fundamental haptic properties [10], and it plays a crucial role for task accomplishment in many scenarios and applications. For example, De Rossi [11] integrated electroactive polymeric materials into wearable garments to endow them with sensing and actuation properties, for applications in post-stroke rehabilitation. Mueller [12] proposed an air-inflatable vest that can be remotely triggered to create a sensation of being hugged. Bau et al. [13] developed a matrix of electromagnetic actuators enclosed in fabric, able to expand and shrink. Sahoo et al. [14] presented a tabletop display providing controlled self-actuated deformation to an elastic fabric surface. The surface is composed of a highly-stretchable pure spandex fabric, which is electrostatically actuated by nine electrodes. More recently, Bianchi et al. [15], [16] proposed a wearable softness display for the fingertip. It controls the stretching state of a fabric to reproduce different stiffness levels, and it can convey, at the same time, softness information, tangential cues, and enable both passive and active haptic exploration. It weights 100 g for 100×60×36 mm dimensions. The same group also applied a similar fabric-based rendering principle at the forearm [17] and arm [18].

A more extensive review of the literature on wearable cutaneous devices for the fingertip can be found in [19], [20].

This paper presents a the application of a 3RRS wearable fingertip device (see Fig. 1) to render the softness of a surface. It is composed of a static upper body and a mobile end-effector: the upper body is located on the nail side of the finger, supporting three small servo motors, and the mobile end-effector is in contact with the finger pulp. The two parts are connected by three articulated legs, actuated by the motors. The end-effector can move toward the user's fingertip and rotate it to simulate contacts with arbitrarily-oriented surfaces. Moreover, a vibrotactile motor placed below the end-effector conveys vibrations to the fingertip. The device was preliminarily introduced in [21], [22]. However, these two works mainly focused on its mechatronic design, mechanical analysis and design, and position control system. In this paper, we will show how the device can be used to render the softness of a surface and, in particular, we will focus on its stiffness control system.

The paper is organized as follows. Section 2 introduces the device and summarizes its main features, and in particular some details on the device mechanical model and on the evaluation of the Jacobian matrix, necessary to evaluate the equivalent stiffness matrix in the actuated joint space. Section 4 describes the main outcomes of device kinematics model and proposes a position control system in which the stiffness can be regulated to render the compliance of a virtual surface. Section 5 shows some experiments in which the proposed control scheme is exploited. Finally, Sec. 6 discusses the obtained results.

2 Device Description

As previously introduced, the wearable fingertip device proposed in this paper has a 3-DoF parallel structure, in which each leg connecting the end-effector to the upper body is composed of two rigid links constrained to each other, the body, and the end-effector, according to a RRS (Revolute-Revolute-Spherical) kinematic chain (see Fig. 2a and 2b). Specifically, three spherical (S) joints connect the distal links of the legs to the end-effector, one revolute (R) joint connects the distal and proximal links of each leg, and another revolute (R) joint connects the proximal link of each leg to the body. The three revolute joints between the proximal links and the body are actuated by the servo motors. In each leg, the axes of the two revolute joints are parallel, so that it constitutes a 2-DoF planar articulated mechanism, constraining the motion of the center of each spherical joint on a plane fixed w.r.t. the body. The mobile end-effector has therefore 3-DoF w.r.t.

Control System	Atmega328
Operating Voltage range	4.8 to 6.0 V
Operating Joints Speed	0.2 s/60° to 0.1 s/60°
Maximum Normal Force	4.7 N
Maximum Roll Angle	$\frac{\pi}{5}$ *rad*
Maximum Pitch Angle	$\frac{\pi}{6}$ *rad*
Maximum Vertical Displacement	15 mm
Frequency vibration range	50 – 240 Hz
Amplitude vibration range	0.05 – 1 g

TABLE 1: Specifications for the proposed 3-DoF cutaneous device.

the body. The proposed device weights 25 g for 35×50×48 mm dimensions.

With respect to the cable-driven fingertip devices presented in [5], [23], [24], this device solves the indeterminacy due to the underactuation of the platform. In fact, the platform is moved through three articulated legs, constraining its motion in a three–dimensional subspace [25]. This mechanical structure decouples position and force control problems, simplifying the control structure with respect to the solution proposed in [5]. The fingertip device is wired to an arm band on the upper arm, that hosts a Raspberry Pi Model B, an Arduino Nano, and two 2 Ah batteries. The arm band is in charge of providing the required power to the device and to manage the wireless communication between the device and an external computer.

For our prototype, shown in Fig. 2a and 1b, we used three HS-5035HD servomotors by Hi-Tech Motors and one 304-101 vibration motor by Precision Microdrives. The stall torques provided by each servomotor allow us to reach a maximum force of 4.7 N at the end-effector. The overall performance and operative parameters of our device are summarized in Table 1.

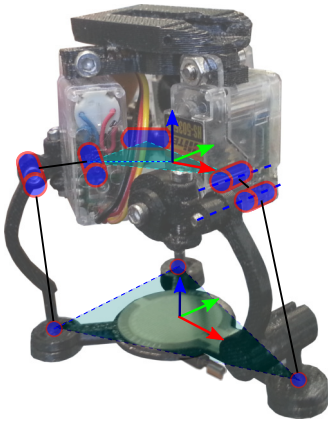

(a) Picture of the device.

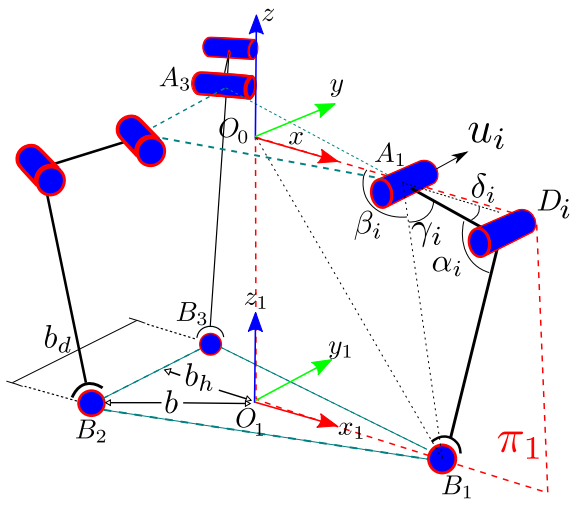

(b) Scheme of the device.

Fig. 2: Kinematic structure of the 3RRS wearable fingertip device. The servo motors move the mobile end-effector toward the user's fingertip and re-angle it to simulate contacts with arbitrarily oriented surfaces. Moreover, a vibrotactile motor placed below the end-effector conveys vibrations to the fingertip.

3 Device Analysis

In this section, we summarise some details on the device mechanical model, in particular on the evaluation of the Jacobian matrix and of the equivalent stiffness matrix, necessary to simulate the contact with surfaces of different compliance values. Further details on the device mechanical analysis, including some numerical simulations, and manipulability evaluation, are available in [21]. In this section, we summarise the main elements of the device mechanical model, necessary to develop the stiffness control system we adopted in the remaining of the paper. A complete analysis of the device kinematics and dynamics is out of the scope of this work; however, we have reported some necessary details in the following, regarding, in particular, the evaluation of the complete Jacobian matrix.

The meaning of the main symbols adopted in this section, representing device geometrical properties, are shown in Fig. 2b. Coherently with the model presented in [21], let us indicate with B_i, $i = \{1,2,3\}$ the centers of the spherical joints on the mobile platform. They define a plane on which we fix the origin O_1 of the frame $S_1 = \langle O_1, x_1, y_1, z_1 \rangle$. Let us then indicate with u_i the unit vectors identifying, for each leg, the direction of the revolute joint axes, and with A_i and D_i, the points indicating the joints connecting each leg to the upper body, and to the middle joint, respectively. On the upper body, we also define a reference frame $S_0 = \langle O_0, x, y, z \rangle$.

The mobile platform will move w.r.t. the upper body according to the rotations imposed by the actuators to the joints passing through A_i and according to the kinematic constraints imposed by the mechanical structure. In particular, since the axes of the revolute joints of each leg are parallel, each B_i and D_i points move on the respective plane, that we indicate with π_i. The overall six dimensional motion of the platform is the composition of a translational and rotational motion, that can be represented by a three dimensional vector $p = [p_x,\ p_y,\ p_z]^{\mathrm{T}}$, containing the coordinates of O_1 w.r.t. S_0, and another three dimensional vector $\varphi = [\psi,\ \theta,\ \phi]^{\mathrm{T}}$, containing the roll ($\psi$), pitch ($\theta$) and yaw ($\phi$) angles that describe the relative orientation between frames S_1 and S_0. From this, we can define a vector $\zeta = [p^{\mathrm{T}}, \varphi^{\mathrm{T}}]^{\mathrm{T}}$ collecting all the six parameters necessary to define position and orientation of the mobile platform with respect to the upper body.

3.1 Inverse kinematics

As previously introduced, each leg connecting the mobile part of the device with the part fixed on the finger, is composed of two links connected to form a RRS (revolute-revolute-spherical) kinematic chain. The mechanism that constitutes the device is therefore 3-DoF, and we can choose three variables to describe its configuration. Since the device has been designed to render the shape and stiffness of virtual and remote objects, a convenient choice for the *independent* variables includes the displacement in the z direction, p_z, and the roll (ψ) and pitch (θ) angles. Let us collect those variables in the vector $\xi = [p_z,\ \psi,\ \theta]^{\mathrm{T}}$. Recalling the rotation matrix expression as a function of the roll/pitch/yaw (RPY) angles, the geometrical dimensions of the device, and the constraints imposed by the legs, we can evaluate the other configuration variables, i.e., yaw angle ϕ, and p_x and p_y components of O_1 coordinates, as

$$\phi = \arctan\left(\frac{(b-b_h)\sin\theta\sin\psi}{b_h(\cos\theta+\cos\psi)}\right), \quad (1)$$

$$p_x = b_h(\cos\phi\cos\theta - \sin\phi\sin\theta\sin\psi - \cos\phi\cos\psi), \quad (2)$$

$$p_y = -b\sin\phi\cos\theta, \quad (3)$$

where b and b_h are the geometrical parameters of the mobile platform, as shown in Fig. 2a.

When controlling the platform, according to the interaction between the fingertip and the environment, we set a reference value for the device platform configuration, ξ_d. Using the relationships in eqs. (1), (2) and (3), we can then evaluate the overall platform configuration corresponding to the desired values of the independent parameters, i.e., $\zeta_d = [p_d^{\mathrm{T}},\ \varphi_d^{\mathrm{T}}]^{\mathrm{T}}$. Through the inverse kinematics, we can then evaluate the corresponding reference values for the actuator rotation angles, collected in the vector $q_d = [q_{1,d},\ q_{2,d},\ q_{3,d}]^{\mathrm{T}}$. For this type of parallel manipulator, the solution of the inverse kinematics problem is straightforward, differently from the direct kinematics one, that, in general, admits multiple solutions.

The coordinates of each B_i point, $i = \{1,2,3\}$, w.r.t. S_0, collected in the three dimensional vectors $b_i = [b_{i,x}, b_{i,y}, b_{i,z}]^{\mathrm{T}}$, can be evaluated as

$$b_i = p + Rb_i^1, \quad (4)$$

where b_i^1 represents the vectors containing the coordinates of B_i points w.r.t. the reference frame S_1, defined on the mobile platform. Since B_i points move on three fixed planes π_i (see Fig. 2b), the following constraint equations hold

$$b_{1,y} = 0, \quad b_{2,x} = \frac{2b_h}{b_d}b_{2,y}, \quad b_{3,x} = -\frac{2b_h}{b_d}b_{3,y}. \quad (5)$$

Eq. (5) introduces three constraints that limit the generic six–dimensional motion of the mobile platform. In particular, since three independent constraints have been introduced, the mobile platform will have three degrees of freedom.

Let us assume that the independent variables $\xi = [p_z,\ \psi,\ \theta]^{\mathrm{T}}$ are defined, and that we need to evaluate the corresponding rotations $q = [q_1,\ q_2,\ q_3]^{\mathrm{T}}$ of the actuated revolute joints in A_i. For a given ξ, it is possible to evaluate, through the constraint equations eq. (1), (2), and (3), the vector p and the rotation matrix R, completing the representation of the mobile platform configuration. Then, from eq. (4), it is possible to evaluate the coordinates of B_i w.r.t. S_0. Finally, angles q_i can be evaluated by solving the triangles $A_iB_iD_i$, in which three edges are known. In particular, the actuator rotation angles q_i can be evaluated as

$$q_i = \alpha_i + \delta_i, \quad (6)$$

where angles α_i and δ_i are as follows

$$\alpha_i = \arctan\left(\frac{s_{iz}}{\sqrt{s_{ix}^2+s_{iy}^2}}\right), \ \delta_i = \arccos\left(\frac{l_1^2+s_i^2-l_2^2}{2l_1|s_i|}\right), \quad (7)$$

where l_1 and l_2 are the lengths of the proximal and distal link of each leg, respectively, i.e., $l_1 = |\overline{D_iA_i}|$, and $l_2 = |\overline{B_iD_i}|$, and $s_i = b_i - a_i$.

3.2 Velocity analysis

We can express the velocities of the B_i points, $i = \{1,2,3\}$, as

$$v_{B_i} = v + \omega \times (b_i - p), \quad (8)$$

where v is the velocity of O_1 and ω is the angular velocity of the mobile platform, expressed w.r.t. the S_0 reference frame. Since the B_i points move on planes perpendicular to the respective u_i directions, which identify the direction of revolute joint axes, the following relationship holds

$$u_i \cdot v_{B_i} = 0,$$

which leads to

$$u_i^{\mathrm{T}}v - u_i^{\mathrm{T}}S(b_i - p)\omega = 0, \quad (9)$$

where the operator $S(\cdot)$, applied to a generic three dimensional vector, gives the corresponding skew matrix. Eq. (9) constitutes an homogeneous linear system with three equations and six unknowns,

$$U\nu = 0, \quad (10)$$

where $\nu = [v^{\mathrm{T}},\ \ \omega^{\mathrm{T}}]^{\mathrm{T}}$ represents the twist of the device mobile platform, and matrix $U \in \mathbb{R}^{3\times 6}$ is defined as

$$U = \begin{bmatrix} u_1^{\mathrm{T}} & -u_1^{\mathrm{T}}S(b_1-p) \\ u_2^{\mathrm{T}} & -u_2^{\mathrm{T}}S(b_2-p) \\ u_3^{\mathrm{T}} & -u_3^{\mathrm{T}}S(b_3-p) \end{bmatrix}. \quad (11)$$

The solutions of this homogeneous system represent, at a given configuration, all the possible twists that can be imposed to the platform.

Since the system has three degrees of freedom, we can express the twist of the platform as a function of three independent velocity components. Similarly to the position analysis described in Sec. 3.1, in our device we want to control the components v_z (component of the velocity in the direction perpendicular to the platform), ω_x (roll velocity), and ω_y (pitch velocity), collected in the vector $\chi = [v_z,\ \omega_x,\ \omega_z]^{\mathrm{T}}$. We collect the remaining components in the vector $\tilde{\chi} = [v_x,\ v_y,\ \omega_z]^{\mathrm{T}}$. It is now clear that

$$\nu = T\begin{bmatrix} \chi \\ \tilde{\chi} \end{bmatrix}, \quad (12)$$

where $T \in \mathbb{R}^{6\times6}$ is a matrix that changes vector component order, specifically

$$T = \begin{bmatrix} 0 & 0 & 0 & 1 & 0 & 0 \\ 0 & 0 & 0 & 0 & 1 & 0 \\ 1 & 0 & 0 & 0 & 0 & 0 \\ 0 & 1 & 0 & 0 & 0 & 0 \\ 0 & 0 & 1 & 0 & 0 & 0 \\ 0 & 0 & 0 & 0 & 0 & 1 \end{bmatrix}. \tag{13}$$

It is worth to observe that, in general, $\chi \neq \dot{\xi}$, and $\nu \neq \dot{\zeta}$. The approximation $\chi \cong \dot{\xi}$ is possible only if rotation angles ψ and θ are small.

We can then rearrange the system in eq. (10) as

$$U_\chi \chi + U_{\tilde{\chi}} \tilde{\chi} = 0, \tag{14}$$

with $U_\chi, U_{\tilde{\chi}} \in \mathbb{R}^{3\times3}$. Assuming that $U_{\tilde{\chi}}$ is non-singular, we can then express

$$\tilde{\chi} = -U_{\tilde{\chi}}^{-1} U_\chi \chi, \tag{15}$$

and, therefore, we can express the device platform twist as a function of the controlled components of the velocity,

$$\nu = H\chi, \tag{16}$$

where $H \in \mathbb{R}^{6\times3}$ is a matrix whose components depend on platform configuration, specifically

$$H = T \begin{bmatrix} I \\ -U_{\tilde{\chi}}^{-1} U_\chi \end{bmatrix}. \tag{17}$$

The velocities of B_i points can also be evaluated considering the articulated mechanism of each leg, as follow

$$v_{Bi} = \omega_i \times (d_i - a_i) + \omega_i' \times (b_i - d_i), \tag{18}$$

where $\omega_i = \dot{q}_i u_i$ are the angular velocities of the links connected to the upper body, actuated by the motors, and ω_i' are the angular velocities of the links connected to the mobile platform, that are not actuated (passive joints). The directions of both ω_i and ω_i' are parallel to u_i (see Fig. 2). From eq. (8) and (18), dot multiplying both sides by $(b_i - d_i)$, we get

$$(b_i - d_i)^{\mathrm{T}} v - (b_i - d_i)^{\mathrm{T}} S(b_i - p)\omega = (b_i - d_i)^{\mathrm{T}} S(d_i - a_i)\omega_i. \tag{19}$$

Collecting the actuator angular velocity magnitudes in a vector $\dot{q} = [\dot{q}_1,\ \dot{q}_2,\ \dot{q}_3]^{\mathrm{T}}$, eq. (19) can be written in matrix form as

$$E\nu = F\dot{q}, \tag{20}$$

where $E \in \mathbb{R}^{3\times6}$ and $F \in \mathbb{R}^{3\times3}$ are defined as

$$E = \begin{bmatrix} (b_i - d_i)^{\mathrm{T}} & (b_i - d_i)^{\mathrm{T}} S(b_i - p) \end{bmatrix}$$

$$F = \mathrm{diag}\begin{bmatrix} (b_i - d_i)^{\mathrm{T}} S(d_i - a_i) u_i \end{bmatrix}, \quad i = 1,2,3.$$

If F is invertible, recalling eq. (16), it is possible to evaluate the actuator velocities $\dot{q}$ as a function of the platform twist ν, i.e.,

$$\dot{q} = \tilde{J}\nu, \tag{21}$$

where $\tilde{J} = F^{-1}E \in \mathbb{R}^{3\times6}$ is the *complete* Jacobian matrix.

If we consider also the constraint in eq. (9), we can define the *constrained* Jacobian matrix $J = \tilde{J}H = F^{-1}EH \in \mathbb{R}^{3\times3}$, relating the actuator angular velocities to the independent twist components, i.e.,

$$\dot{q} = J\chi. \tag{22}$$

If the mechanism is not in a singular configuration, i.e., if J is full-rank, eq. (22) can be inverted to solve the direct differential kinematic problem, i.e. $\chi = J^{-1}\dot{q}$.

3.3 Statics

Let us consider now the static equilibrium of the device. We indicate with $w = [f,\ m]^{\mathrm{T}} \in \mathbb{R}^6$ the wrench applied to the mobile platform, where f is the resulting force applied to the mobile platform and m is the resulting moment evaluated w.r.t. O_1. This wrench represents the resultant of the interaction between the platform and the fingertip, dependent on the fingertip skin deformation. The skin deformation and the stress distribution are related by an impedance relationship that is non-linear and dependent on several parameters [26], [27], [28], [29].

Let us indicate with $\tau = [\tau_1,\ \tau_2,\ \tau_3]^{\mathrm{T}}$ the torques applied by the actuators to the links connected to the upper body.

Considering a virtual displacement of the mobile platform, $\delta\zeta$, generated by a small variation of actuator joint angles, δq, according to the Principle of Virtual Works, the following relationship can be written

$$\delta\zeta^{\mathrm{T}} w = \delta q^{\mathrm{T}} \tau. \tag{23}$$

The components of $\delta\zeta$ are not independent, since the device has 3-DoF. Recalling the constraint relationships in eq. (16) and eq. (22), we get

$$\delta\chi^{\mathrm{T}} H^{\mathrm{T}} w = \delta\chi^{\mathrm{T}} J^{\mathrm{T}} \tau. \tag{24}$$

Since $\delta\chi$ components are independent, this relationship holds for any $\delta\chi$ only if

$$H^{\mathrm{T}} w = J^{\mathrm{T}} \tau, \tag{25}$$

and, consequently, if the Jacobian matrix J is invertible, i.e., if the device is in a nonsingular configuration,

$$\tau = J^{-\mathrm{T}} H^{\mathrm{T}} w. \tag{26}$$

4 Device Control

4.1 Equivalent stiffness evaluation

The objective of our stiffness control system is to simulate contact with a surface of given stiffness, represented by the matrix K_d. Indicating with

$$K_p = \mathrm{diag}(k_x, k_y, k_z), \quad K_\varphi = \mathrm{diag}(k_\psi, k_\theta, k_\phi), \tag{27}$$

the desired translational stiffness and the desired rotational stiffness, respectively, the desired stiffness matrix is defined as

$$K_d = \mathrm{diag}(K_p, K_\varphi). \tag{28}$$

When the platform is in a generic configuration ζ, the corresponding wrench that has to be applied to the fingertip is given by

$$w = K_d \Delta\zeta, \tag{29}$$

where $\Delta\zeta = \zeta - \zeta_0$ and ζ_0 is an initial configuration corresponding to $w = 0$. $\Delta\zeta$ is related to a variation of the independent variables $\Delta\xi$ through the relationships in eq. (1), (2), and (3). For small values of $\Delta\zeta$, we can use the approximation

$$\Delta\zeta = H\Delta\xi, \tag{30}$$

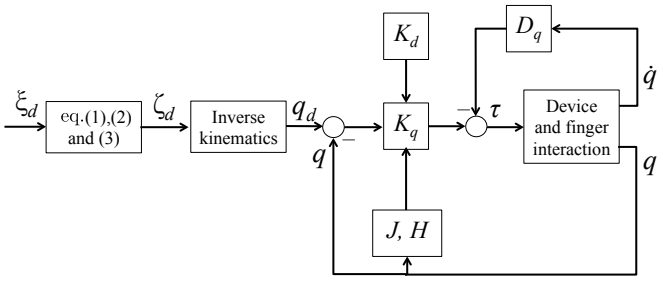

Fig. 3: Position control of the platform with adaptable contact stiffness simulation. The proportional gain matrix K_d is evaluated as a function of the stiffness that has to be simulated and the platform configuration, through the Jacobian matrix J and the matrix H, relating dependent and independent components of platform configuration vector.

where H is defined in eq. (16). Assuming for the device actuator an impedance (stiffness) control system, the torque applied by device actuators, necessary to balance the wrench $-w$ that the fingertip exerts on the platform, can be expressed as

$$\tau = K_q \Delta q, \tag{31}$$

where $\Delta q = q - q_0$ and q_0 represents the joint configuration corresponding to ζ_0. For small values of Δq we can use the approximation

$$\Delta q = J \Delta \xi. \tag{32}$$

where J is defined in eq. (21). By substituting eq. (29), (30), (31), and (32) in eq. (26), we get

$$K_q J \Delta \xi = J^{-\mathrm{T}} H^{\mathrm{T}} K_d H \Delta \xi. \tag{33}$$

Since this relationship holds for any $\Delta\xi$, whose components can be set independently, the following matrix equality can be set

$$K_q J = J^{-\mathrm{T}} H^{\mathrm{T}} K_d H. \tag{34}$$

Finally, assuming again a non-singular configuration and that the Jacobian matrix J is invertible, we can right-multiply both sides of eq. (34) by J^{-1}. We then obtain the expression that allows to evaluate the stiffness matrix in the joint space, K_q, corresponding to a given stiffness matrix in the operative space of the device platform, K_d:

$$K_q = J^{-\mathrm{T}} H^{\mathrm{T}} K_d H J^{-1}. \tag{35}$$

It is worth to observe that K_q components depend on the stiffness K_d that has to be rendered, but also on the platform configuration, that affects the values of matrices J and H.

4.2 Control system description

Let us consider a Virtual Reality (VR) scenario, in which we haptically render the stiffness of different virtual surfaces, e.g., grasping and interacting with surfaces that have different mechanical properties. For the sake of clarity, let us consider only one cutaneous device. However, thanks to the wearability of our system, this framework can be easily extended to multi-contact interactions (see the multi-contact experience of Sec. 5.2). Let us also assume the availability of a hand motion capture system, able to measure the configuration (position and orientation) of the $\{S_0\}$ frame, introduced at the beginning of Sec. 3. This measure is adopted to render the position and orientation of the user's fingertip avatar in the VR environment. A contact detection algorithm is then used to recognize the interactions between the haptic-equipped fingertip and the virtual objects, i.e., the desired configuration of the device's platform ξ_d with respect to $\{S_0\}$. Let us assume K_d to be the stiffness matrix of the simulated contact surface. The complete position and orientation vector ζ_d is evaluated by means of eqs. (1), (2), and (3). Reference values for the device actuators angular positions q_d can be evaluated by applying the inverse kinematic procedure detailed in Sec. 3. These reference values q_d are then compared with the angles measured by the actuator encoders, $q = [q_1,\ q_2,\ q_3]^{\mathrm{T}}$, and their difference is sent to a position controller with a proportional-derivative (PD) scheme. The proportional term K_q is dynamically evaluated to simulate the stiffness of the virtual surface, as a function of the desired stiffness K_d and of the platform configuration, i.e., matrices H and J, according to eq. (35).

Moreover, the derivative term $D_q \in \mathbb{R}^{3\times3}$ is set to have a suitable damping in system dynamical behavior. In future developments of this work, also $D_q \in \mathbb{R}^{3\times3}$ will be dynamically regulated to simulate a viscous behaviour in the interaction with the virtual environment. Finally, the torque τ generated by actuators is evaluated as

$$\tau = K_q (q_d - q) + D_q (\dot{q}_d - \dot{q}). \tag{36}$$

A simplified block diagram of the proposed stiffness control algorithm is shown in Fig. 3.

5 Experimental Evaluation

We carried two experiments to test the effectiveness of our wearable haptic device and its level of wearability. In the first experiment we aimed at evaluating the effectiveness of our wearable haptic device in rendering stiffness information, while in the second experiment we focused on the evaluation of its immersiveness and wearability.

5.1 Experiment #1: stiffness discrimination experiment

In order to test the effectiveness of our wearable haptic device in rendering stiffness information, we carried out a stiffness discrimination experiment using the same-different procedure of TSD (theory of signal detection) [30]. This technique enables us to evaluate the differential stiffness threshold for our device. The differential threshold can be defined as "the smallest amount of stimulus change necessary to achieve some criterion level of performance in a discrimination task" [30]. It gives us information about how different two displacements provided with our device need to be in order to be perceived as different by a human user. This threshold is often referred to as just-noticeable difference or JND. The differential threshold of a perceptual stimulus reflects also the fact that people are usually more sensitive to changes in weak stimuli than they are to similar changes in stronger or more intense stimuli. The German physician Ernst Heinrich Weber proposed the simple proportional law $JND = kI$, suggesting that the differential threshold increases with increasing the stimulus intensity I. Constant k is thus referred to as "Weber's fraction".

5.1.1 Setup

The experimental setup is composed of two wearable fingertip devices attached to the end-effectors of two 3-DoF Falcon haptic interfaces (Novint Technologies, USA), as shown in Fig. 4. The Falcon interfaces are placed so that the centers of their end-effectors are at a distance of 13 cm in the nominal position,

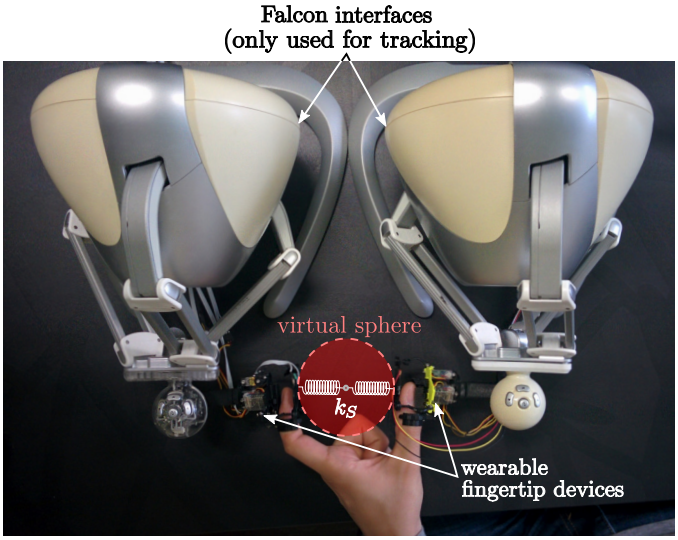

Fig. 4: Experimental setup. Two wearable devices are attached to the end-effectors of two Falcon interfaces, with the end-effectors facing each other. The Falcon interfaces are only used to track the position of the fingers and do not provide any external force to the user.

and the wearable devices are mounted to have the end-effectors of the devices facing each other. Each Falcon has a workspace of 11×12.5×13 cm and a tracking accuracy of 0.06 mm [31]. Subjects were blindfolded and asked to wear the two wearable fingertip devices on the thumb and index finger of their right hand.

5.1.2 Methods

Eighteen participants (15 males, 3 females, age range 22 – 37) took part to the experiment, all of whom were right-handed. Nine of them had previous experience with haptic interfaces. None of the participants reported any deficiencies in their perception abilities and they were all naïve as to the purpose of the study.

We evaluated the differential threshold for stiffness discrimination using the same-different procedure [30]. Each trial involved interacting, in succession, with two virtual spheres rendered between the two wearable devices (see Fig. 4). Subjects were asked to judge, on each trial, if the stiffness of the two virtual spheres was different or the same. The hit rate p_h corresponded to the percentage of correct responses given by a subject ("yes, the spheres are different") when the two objects had different stiffness, while the false alarm rate p_f corresponded to the percentage of incorrect responses ("yes, the spheres are different") when the stiffness of the two objects were the same [30]. No visual feedback on the virtual sphere was provided.

The two Falcon haptic interfaces were only used to track the position of the fingers and did not provide any external force to the user, i.e., they were programmed to provide only gravity compensation. We decided to use these grounded interfaces, instead of, e.g., a wireless motion tracking system, to enable a more precise tracking of our devices. We will focus on the evaluation of the wearability and portability of our system in the experiment of Sec. 5.2.

We evaluated the differential threshold for stiffness discrimination when employing

(S) cutaneous feedback provided only by the servo motors of the wearable device (no vibrations),

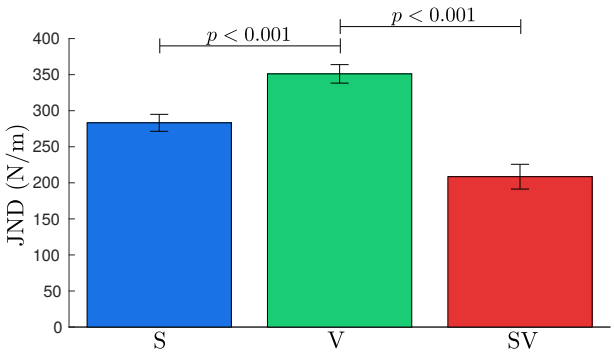

Fig. 5: Differential threshold for stiffness discrimination. Mean and and 95% confidence interval are plotted for condition providing cutaneous feedback only by the servo motors (S), only by the vibrotactile motor (V), and both by the servo motors and the vibrotactile motor (SV).

(V) cutaneous feedback provided only by the vibrotactile motor of the wearable device (platform not moving),

(SV) cutaneous feedback provided both by the servo motors and the vibrotactile motor of the wearable device.

In condition S, the servo motors move the end-effector to render the contact with the virtual sphere, and the vibrotactile motor is not active. The interaction is designed according to the god-object model [32], and the magnitude of the force applied at the fingertip is evaluated as

$$f_S = k_S \Delta x, \tag{37}$$

where Δx is the penetration of the finger inside the virtual object and k_S is the simulated stiffness constant. More in detail, in this experiment the desired translational stiffness matrix K_p introduced in eq. (27) is defined as $K_p = k_S I_{3\times3}$, where $I_{3\times3}$ identifies the three dimensional identity matrix. The same numerical values were assumed for the sake of simplicity also for the K_φ matrix introduced in eq. (27), even if its values are represented with different units. Once the desired stiffness K_d matrix is set as in eq. (28), the equivalent K_q matrix can be evaluated according to eq. (35).

In condition V, the vibrotactile motor provides a 100-ms vibration burst when the finger contacts the virtual sphere. The amplitude A_V of the vibration is proportional to the stiffness of the virtual sphere [33], i.e.,

$$A_V = \left(\frac{k_S}{1500} + 0.4\right) G, \tag{38}$$

where G is the acceleration from gravity. In this case, the servo motors are not active, and the mobile platform always contacts the fingertip. Providing a vibration burst of fixed duration on making/breaking contact events has been proved to improve the performance of several (tele)manipulation tasks [34], [35], [36], [37]. Moreover, amplitude (and frequency) of the contact vibration has been proved to generally increase with increasing stiffness of the touched object [38].

Finally, in condition SV, cutaneous feedback is provided both by the servo motors and the vibrotactile motor, as indicated in eqs. (37) and (38).

Each subject carried out three series of trials, in which the virtual sphere stiffness k_S assumed two different values, $k_S = k_{a,*}$

and $k_S = k_b$, where $k_{a,*}$ and k_b assumed the following numerical values:

(i) $k_{a,1} = 500$ N/m and $k_b = 900$ N/m ($k_{a,1} - k_b = 400$ N/m) for Series 1,
(ii) $k_{a,2} = 600$ N/m and $k_b = 900$ N/m ($k_{a,2} - k_b = 300$ N/m) for Series 2,
(iii) $k_{a,3} = 700$ N/m and $k_b = 900$ N/m ($k_{a,3} - k_b = 200$ N/m) for Series 3.

Each series consisted of 36 repetitions of the stiffness discrimination task, with 12 trials for each feedback condition. The entire experiment lasted approximately 35 minutes.

On each repetition of each series, two virtual spheres with random stiffness ($k_{a,*}$ or k_b) were rendered, i.e., the probability of interacting with a pair of objects with same (different) stiffness was 0.5. The order of presentation of the sequence of series and conditions was different for each subject, in order to minimize learning and fatigue effects.

5.1.3 Results

False alarm and hit rate were converted to z scores of the normal distribution [30], [39]. The sensitivity index d' was then calculated as the difference

$$d' = z_h - z_f.$$

According to the criterion commonly adopted [1], [5], [30], the discrimination threshold can be defined as the difference between the stiffness for which $d' = 1$. The threshold was computed for each subject for each condition S, V, and SV, assuming a linear proportionality between the values of d'.

The overall JND was then computed as the mean of the values obtained for all the subjects. Fig. 5 shows the average JND and 95% confidence interval for each condition. The collected data of each condition passed the Shapiro-Wilk normality test and the Mauchly's test of sphericity. A repeated-measures ANOVA showed a statistically significant difference between the means of the three feedback conditions ($F_{2,34} = 47.153$, $p < 0.001$, a = 0.05). Post-hoc analysis (Games-Howell post-hoc test) revealed statistically significant in S vs. V ($p < 0.001$) and V vs. SV ($p < 0.001$), while S vs. SV fell short of significance ($p = 0.154$). Time needed to complete the given tasks was recorded as well. No statistically significant difference was found.

In addition to the quantitative evaluation reported above, we also measured the users' experience. Immediately after the experiment, subjects were asked to report the effectiveness of each feedback condition in completing the given task using bipolar Likert-type nine-point scales. Condition S scored 6.7 out of 9, condition V scored 3.7 out of 9, and condition SV scored 7.6 out of 9. Although we registered no significant difference between conditions S and SV, subjects appreciated the capability of the vibrotactile bursts to effectively notify the making contact with the virtual surface.

5.2 Experiment #2: interaction with a virtual immersive environment

In order to test the level of wearability of our cutaneous device, we carried out a second experiment, where subjects are requested to interact with a virtual immersive environment. This experience has been inspired by the experiments carried out in [40], [41]. Since here we focus on the wearability aspect of our system, we substituted the two Falcon interfaces with the unobtrusive Leap Motion tracking system. The interaction forces are still computed according to the stiffness rendering algorithm of Sec. 4.

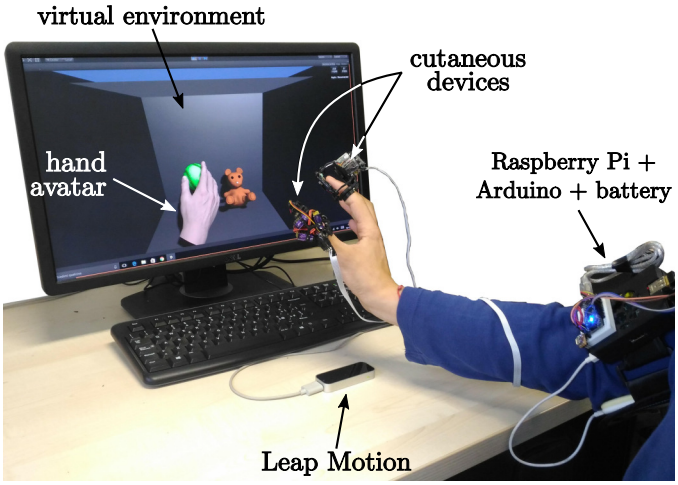

Fig. 6: Experimental setup. Subjects were asked to interact with the virtual environment while wearing two wearable cutaneous devices, one on the thumb and one on the index finger. The virtual environment is composed of a baseball (being grasped in the picture) and a teddy bear. Interaction forces in the virtual environment are provided to the user by the cutaneous device as indicated in Sec. 4.

5.2.1 Setup and Methods

The experimental setup is composed of a Leap Motion controller, one wearable fingertip device, and a virtual environment. The Leap Motion controller is a small USB peripheral device that uses two monochromatic IR cameras and three infrared LEDs to track the position of the fingertip in 3-D space. It observes a hemispherical area up to a distance of 1 m with an average accuracy of 0.7 mm [42]. Subjects are required to wear two fingertip devices on the thumb and index finger of their right hand, and interact with the virtual environment (see Fig. 6). The subjects hand pose is tracked using the Leap Motion controller and a virtual hand mimicked the subjects hand pose in the virtual environment. Every time the index finger comes in contact with a virtual object, the cutaneous device applies a suitable amount of force to the fingertip. Interaction forces in the virtual environment are computed using a virtual proxy approach [43] and were provided by the cutaneous device as indicated in Sec. 4. The virtual environment is composed of a baseball and a teddy bear, as shown in Fig. 6.

Twelve participants (10 males, 2 females, age range 21 – 35) took part to the experiment, all of whom were right-handed. Eight of them had previous experience with haptic interfaces. None of the participants reported any deficiencies in their perception abilities and they were all naïve as to the purpose of the study.

The task consisted of interacting with the two virtual objects for 5 minutes, either wearing two wearable cutaneous devices (condition C, as in Fig. 6) or barehanded (condition N).

5.2.2 Results

We evaluated the immersiveness of the haptic-enabled virtual reality scenario through the Usefulness, Satisfaction, and Ease of use (USE) questionnaire [44], asking subjects to compare the experience while wearing the wearable devices vs. bare hand. Our

TABLE 2: Experiment #2. Usefulness, Satisfaction, and Ease of use (USE) questionnaire results.

QA. Usefulness (condition C with respect to condition N)	
1. It helps me be more effective.	8.3 ± 0.9
2. It helps me be more productive.	7.9 ± 1.2
3. It is useful.	6.8 ± 1.3
4. It makes the things I want to accomplish easier to get done.	8.1 ± 0.7

Experiment in condition C (statistically different values in red)	
QB. Ease of use	
1. It is easy to use.	3.4 ± 1.9
2. It is simple to use.	7.2 ± 1.5
3. It is user friendly.	6.3 ± 1.4
4. Using it is effortless.	5.5 ± 1.2
5. I can use it without written instructions.	2.6 ± 1.4
6. I don't notice any inconsistencies as I use it.	6.7 ± 7.6
7. Both occasional and regular users would like it.	7.3 ± 0.6
8. I can recover from mistakes quickly and easily.	7.3 ± 1.2
9. I can use it successfully every time.	4.1 ± 1.6
QC. Ease of learning	
1. I learned to use it quickly.	4.3 ± 1.4
2. It is easy to learn to use it.	5.9 ± 1.4
3. I quickly became skillful with it.	6.4 ± 0.9
QD. Satisfaction	
1. I am satisfied with it.	7.1 ± 1.4
2. It is fun to use.	8.7 ± 0.5
3. It works the way I want it to work.	7.3 ± 1.4
4. It is wonderful.	7.6 ± 1.6
5. It is pleasant to use.	7.2 ± 1.3

Experiment in condition N (statistically different values in red)	
QB. Ease of use	
1. It is easy to use.	4.2 ± 2.2
2. It is simple to use.	6.7 ± 2.0
3. It is user friendly.	7.1 ± 1.9
4. Using it is effortless.	5.8 ± 0.7
5. I can use it without written instructions.	5.4 ± 1.4
6. I don't notice any inconsistences as I use it.	7.6 ± 0.8
7. Both occasional and regular users would like it.	5.2 ± 1.7
8. I can recover from mistakes quickly and easily.	7.5 ± 1.2
9. I can use it successfully every time.	4.4 ± 1.6
QC. Ease of learning	
1. I learned to use it quickly.	6.9 ± 1.6
2. It is easy to learn to use it.	7.7 ± 1.3
3. I quickly became skillful with it.	6.8 ± 0.6
QD. Satisfaction	
1. I am satisfied with it.	4.8 ± 1.4
2. It is fun to use.	6.2 ± 1.2
3. It works the way I want it to work.	6.7 ± 0.5
4. It is wonderful.	5.5 ± 1.5
5. It is pleasant to use.	7.1 ± 0.7

USE questionnaire is composed of 21 Likert-type questions. It contained a set of assertions, where a score of 9 was described as "completely agree" and a score of 1 as "completely disagree" with the assertion. Questions and results are reported in Table 2. The first set of questions (QA in Table 2) considered the usefulness of having the wearable cutaneous devices (C) with respect to not having any force feedback (N). The other three sets of questions (QB, QC, and QD in Table 2) were asked separately for both conditions. In order to determine whether the data registered in sets B, C, and D differ between the two feedback conditions, we ran seventeen Wilcoxon signed-rank tests (significance level alpha = 0.05), one for each question. The Wilcoxon signed-rank test is the non-parametric equivalent of the more popular paired t-test. The latter is not appropriate here since the dependent variable was measured at the ordinal level. The analysis revealed significant statistical difference between answers QB5 ($p = 0.050$), QB6 ($p = 0.013$), QB7 ($p = 0.012$), QC1 ($p = 0.003$), QC2 ($p = 0.016$), QD1 ($p = 0.010$), QD2 ($p = 0.015$), and QD4 ($p = 0.005$). Answers that resulted statistically significantly different are reported in red in Table 2.

We also asked which condition the subjects preferred. All subjects preferred the condition where they were wearing the wearable cutaneous devices. However, four subjects out of twelve complained that, while wearing the wearable devices, the tracking of the fingertip seemed less accurate with respect to interacting with the environment barehanded.

6 Discussion and Conclusions

This work presented the application of a 3RRS wearable fingertip device for stiffness discrimination. Three servo motors move a mobile end-effector toward the user's fingertip and re-angle it to simulate contacts with arbitrarily oriented surfaces. Moreover, a vibrotactile motor conveys vibrations to the fingertip. The device was preliminary introduced in [21], [22]. In this paper, we have extended the analysis and evaluation of the device with a novel stiffness control system and an in-depth kinematics analysis. Moreover, in order to test the effectiveness and wearability of our wearable haptic device, we carried out two experiments.

Stiffness discrimination experiment. The first experiment tested the capability of our device in differentiating stiffness information. We considered three feedback conditions: cutaneous feedback provided only by the servo motors (S), only by the vibrotactile motor (V), and both by the servo motors and the vibrotactile motor (SV). In the best condition, SV, subjects were able to differentiate

values of stiffness different by 208.5 $\pm$ 17.2 N/m (mean $\pm$ 95% confidence interval). Surprisingly, adding vibrotactile feedback did not significantly improved the performance of the stiffness discrimination task. However, subjects appreciated the capability of the vibrations to effectively notify the making contact with the virtual surface. The Weber fraction (*JND/I*, see Sec. 5.1.2) for conditions S, V, and SV is 31.5%, 39.0%, and 23.2%, respectively, which is in agreement with previous results in the literature. For example, Lècuyer et al. [45] used a passive isometric input device, together with visual feedback, to provide the operator with pseudo-haptic feedback. The Weber Fraction for stiffness between a real spring and a spring rendered using the isometric input device was 16%. Genecov et al. [46] presented a tactile display capable of simultaneously and independently controlling its stiffness and geometry via particle jamming and pneumatic actuation. The Weber Fraction for stiffness was also 16%. Gurari et al. [47] compared the Weber fraction for human perception of stiffness among three conditions: vision, proprioceptive motion feedback, and their combination. Results gave average Weber fractions of 5.6% for vision, 3.6% for proprioception, and 3.9% for their combination. As expected, our performance is sligthly worse with respect to [45], [46] and significantly worse than [47]. This can be justified by the fact that we are using wearable tactile interfaces with limited actuation and sensing capabilities, and no visual feedback was provided.

In this experiment, to precisely track the position of the fingers, we used two Falcon interfaces (see Fig. 4), able to guarantee a high tracking accuracy (i.e., more than 10 times higher than the Leap Motion used in the second experiment). However, of course, this choice severely reduced the workspace of the system and did not enable us to evaluate the portability and wearability of our system, which is one of the main points of our work. Moreover, the Falcon interfaces, even when commanded to provide no external force, shows an internal stiffness and friction that is unwittingly displayed to the user. However, since this effect was present in all the considered comparisons, we expect it to have negligible effect in the final computation of the differential thresholds.

Immersive environment experiment. The second experiment tested the effectiveness of our device in an immersive virtual reality scenario, focusing on its wearability and portability. All subjects preferred the experience while being provided with cutaneous feedback. Moreover, cutaneous feedback made the interaction more satisfactory (question QD1), more fun to use (QD2), and more "wonderful" (QD4). On the other hand, as expected, wearing the two devices made the task more difficult to learn (QB5, QC1, QC2). Indeed, most of the subjects had no previous experience with wearable interfaces, and they had to get used to wearing them before starting to truly appreciate the additional information provided. In fact, as mentioned above, after this initial setback, all subjects preferred using the system with the cutaneous devices. Finally, subjects complained that the fingertip tracking worked better when using the system barehanded (QB6). These results show that the proposed wearable solution is definitely well-received and well-appreciated. However, there is still some work to be done to improve the wearability of these systems and the quality of the tracking.

Future Work. In the next future, we are planning to integrate our fingertip device with a compact and lightweight finger exoskeleton, able to provide kinesthetic feedback to the PIP and DIP joints. In order to improve the tracking of fingers wearing cutaneous devices, we will also consider using more sophisticated tracking systems, such as the V:120 Trio by OptiTrack, or placing the devices on other parts of the hand. A promising solution is moving the device from the fingertip to the proximal phalanx, similarly to what has been done in [48], [49], [50]. Moreover, we are also considering the possibility of including an Inertial Measurement Unit (IMU) unit directly on the cutaneous device, in order to combine the information coming from the external tracker (e.g., a Leap Motion) together with the information captured by the IMU. A similar approach is currently being used by the company GoTouchVR for their wearable fingertip device [20]. Finally, to improve the immersiveness of the virtual environment, we will consider using a Virtual Reality headset, such as an Oculus Rift Head-Mounted Display (HMD). We are also interested in studying how amplitude *and* duration of vibration bursts affect the sensation of making and breaking contact with virtual objects in wearable haptics.

REFERENCES

[1] A. Frisoli, M. Solazzi, F. Salsedo, and M. Bergamasco, "A fingertip haptic display for improving curvature discrimination," *Presence: Teleoperators and Virtual Environments*, vol. 17, no. 6, pp. 550–561, 2008.

[2] M. Solazzi, A. Frisoli, and M. Bergamasco, "Design of a cutaneous fingertip display for improving haptic exploration of virtual objects," in *Proc. of IEEE International Symposium on Robots and Human Interactive Communications*, 2010, pp. 1–6.

[3] ——, "Design of a novel finger haptic interface for contact and orientation display," in *Proc. of IEEE Haptics Symposium*, 2010, pp. 129–132.

[4] M. Gabardi, M. Solazzi, D. Leonardis, and A. Frisoli, "A new wearable fingertip haptic interface for the rendering of virtual shapes and surface features," in *2016 IEEE Haptics Symposium (HAPTICS)*, 2016, pp. 140–146.

[5] D. Prattichizzo, F. Chinello, C. Pacchierotti, and M. Malvezzi, "Towards wearability in fingertip haptics: a 3-dof wearable device for cutaneous force feedback," *IEEE Transactions on Haptics*, vol. 6, no. 4, pp. 506–516, 2013.

[6] D. Tsetserukou, S. Hosokawa, and K. Terashima, "Linktouch: A wearable haptic device with five-bar linkage mechanism for presentation of two-dof force feedback at the fingerpad," in *Proc. IEEE Haptics Symposium (HAPTICS)*, 2014, pp. 307–312.

[7] K. Minamizawa, S. Fukamachi, H. Kajimoto, N. Kawakami, and S. Tachi, "Gravity grabber: wearable haptic display to present virtual mass sensation," in *Proc. of ACM Special Interest Group on Computer Graphics and Interactive Techniques*, 2007, pp. 8–es.

[8] D. Leonardis, M. Solazzi, I. Bortone, and A. Frisoli, "A wearable fingertip haptic device with 3 dof asymmetric 3-RSR kinematics," in *Proc. IEEE World Haptics Conference (WHC)*, 2015, pp. 388–393.

[9] A. Girard, M. Marchal, F. Gosselin, A. Chabrier, F. Louveau, and A. Lécuyer, "Haptip: Displaying haptic shear forces at the fingertips for multi-finger interaction in virtual environments," *Frontiers in ICT*, vol. 3, p. 6, 2016.

[10] W. M. B. Tiest and A. M. Kappers, "Cues for haptic perception of compliance," *IEEE Transactions on Haptics*, vol. 2, no. 4, pp. 189–199, 2009.

[11] D. De Rossi, F. Carpi, F. Lorussi, E. P. Scilingo, and A. Tognetti, "Wearable kinesthetic systems and emerging technologies in actuation for upperlimb neurorehabilitation," in *Proc. Annual International Conference of the IEEE Engineering in Medicine and Biology Society*, 2009, pp. 6830–6833.

[12] F. Mueller, F. Vetere, M. R. Gibbs, J. Kjeldskov, S. Pedell, and S. Howard, "Hug over a distance," in *Proc. ACM CHI Conference on Human Factors in Computing Systems*, 2005, pp. 1673–1676.

[13] O. Bau, U. Petrevski, and W. Mackay, "Bubblewrap: a textile-based electromagnetic haptic display," in *CHI'09 Extended Abstracts on Human Factors in Computing Systems*, 2009, pp. 3607–3612.

[14] D. R. Sahoo, K. Hornbæk, and S. Subramanian, "Tablehop: An actuated fabric display using transparent electrodes," in *Proceedings of the 2016 CHI Conference on Human Factors in Computing Systems*, 2016, pp. 3767–3780.

[15] M. Bianchi, "A fabric-based approach for wearable haptics," *Electronics*, vol. 5, no. 3, p. 44, 2016.

[16] M. Bianchi, E. Battaglia, M. Poggiani, S. Ciotti, and A. Bicchi, "A wearable fabric-based display for haptic multi-cue delivery," in *2016 IEEE Haptics Symposium (HAPTICS)*, 2016, pp. 277–283.
[17] M. Bianchi, G. Valenza, A. Serio, A. Lanata, A. Greco, M. Nardelli, E. P. Scilingo, and A. Bicchi, "Design and preliminary affective characterization of a novel fabric-based tactile display," in *2014 IEEE Haptics Symposium (HAPTICS)*, 2014, pp. 591–596.
[18] S. Casini, M. Morvidoni, M. Bianchi, M. Catalano, G. Grioli, and A. Bicchi, "Design and realization of the cuff-clenching upper-limb force feedback wearable device for distributed mechano-tactile stimulation of normal and tangential skin forces," in *Proc. IEEE/RSJ International Conference on Intelligent Robots and Systems (IROS)*, 2015, pp. 1186–1193.
[19] C. Pacchierotti, *Cutaneous haptic feedback in robotic teleoperation*, ser. Springer Series on Touch and Haptic Systems. Springer International Publishing, 2015.
[20] C. Pacchierotti, S. Sinclair, M. Solazzi, A. Frisoli, V. Hayward, and D. Prattichizzo, "Wearable haptic systems for the fingertip and the hand: taxonomy, review, and perspectives," *IEEE Transactions on Haptics*, 2017.
[21] F. Chinello, M. Malvezzi, C. Pacchierotti, and D. Prattichizzo, "Design and development of a 3rrs wearable fingertip cutaneous device," in *Proc. IEEE/ASME International Conference on Advanced Intelligent Mechatronics*, 2015, pp. 293–298.
[22] F. Chinello, C. Pacchierotti, M. Malvezzi, and D. Prattichizzo, "A novel 3rrs wearable fingertip cutaneous device for virtual interaction," in *Proc. Asia Haptics*, 2016.
[23] C. Pacchierotti, L. Meli, F. Chinello, M. Malvezzi, and D. Prattichizzo, "Cutaneous haptic feedback to ensure the stability of robotic teleoperation systems," *International Journal of Robotics Research. In Press*, 2015.
[24] C. Pacchierotti, D. Prattichizzo, and K. J. Kuchenbecker, "Cutaneous feedback of fingertip deformation and vibration for palpation in robotic surgery," *IEEE Transactions on Biomedical Engineering*, vol. 63, pp. 278–287, 2016.
[25] J.-P. Merlet, *Parallel robots*. Springer Science & Business Media, 2006, vol. 128.
[26] W. R. Provancher, M. R. Cutkosky, K. J. Kuchenbecker, and G. Niemeyer, "Contact location display for haptic perception of curvature and object motion," *The International Journal of Robotics Research*, vol. 24, no. 9, pp. 691–702, 2005.
[27] Q. Wang and V. Hayward, "In vivo biomechanics of the fingerpad skin under local tangential traction," *Journal of Biomechanics*, vol. 40, pp. 851–860, 2007.
[28] M. J. Adams, S. A. Johnson, P. Lefèvre, V. Lévesque, V. Hayward, T. André, and J. L. Thonnard, "Finger pad friction and its role in grip and touch," *Journal of The Royal Society Interface*, vol. 10, no. 80, 2013.
[29] M. Wiertlewski and V. Hayward, "Mechanical behavior of the fingertip in the range of frequencies and displacements relevant to touch," *Journal of biomechanics*, vol. 45, no. 11, pp. 1869–1874, 2012.
[30] G. Gescheider, *Psychophysics: the fundamentals*. Lawrence Erlbaum, 1997.
[31] R. Mason and R. Manduchi, "Haptic modeling of a street intersection using the novint falcon," 2008.
[32] C. B. Zilles and J. K. Salisbury, "A constraint-based god-object method for haptic display," in *Proc. IEEE/RSJ International Conference on Intelligent Robots and Systems*, vol. 3, 1995, pp. 146–151.
[33] Precision Microdrives Ltd., "4 mm vibration motor - 11 mm type - operating voltage 3 V (model 304-101)," https://www.precisionmicrodrives.com/product/304-101-4mm-vibration-motor-11mm-type, 2016.
[34] C. Cipriani, J. L. Segil, F. Clemente, B. Edin *et al.*, "Humans can integrate feedback of discrete events in their sensorimotor control of a robotic hand," *Experimental brain research*, vol. 232, no. 11, pp. 3421–3429, 2014.
[35] I. Hussain, G. Salvietti, L. Meli, C. Pacchierotti, D. Cioncoloni, S. Rossi, and D. Prattichizzo, "Using the robotic sixth finger and vibrotactile feedback for grasp compensation in chronic stroke patients," in *Proc. IEEE International Conference on Rehabilitation Robotics (ICORR)*, 2015, pp. 67–72.
[36] C. Pacchierotti, F. Ongaro, F. van den Brink, C. Yoon, D. Prattichizzo, D. Gracias, and S. Misra, "Steering and control of miniaturized untethered soft magnetic grippers with haptic assistance," *IEEE Transactions on Automation Science and Engineering. In Press*, 2017.
[37] L. Meli, C. Pacchierotti, and D. Prattichizzo, "Experimental evaluation of magnified haptic feedback for robot-assisted needle insertion and palpation," *International Journal of Medical Robotics and Computer Assisted Surgery*, 2017.
[38] A. M. Okamura, J. T. Dennerlein, and R. D. Howe, "Vibration feedback models for virtual environments," in *Proc. IEEE International Conference on Robotics and Automation*, 1998, pp. 674–679.
[39] H. Stanislaw and N. Todorov, "Calculation of signal detection theory measures," *Behavior Research Methods*, vol. 31, no. 1, pp. 137–149, 1999.
[40] S. Scheggi, L. Meli, C. Pacchierotti, and D. Prattichizzo, "Touch the virtual reality: using the leap motion controller for hand tracking and wearable tactile devices for immersive haptic rendering," in *Proc. ACM Special Interest Group on Computer Graphics and Interactive Techniques Conference, SIGGRAPH*, Los Angeles, California, USA, 2015.
[41] L. Meli, S. Scheggi, C. Pacchierotti, and D. Prattichizzo, "Wearable haptics and hand tracking via an rgb-d camera for immersive tactile experiences," in *Proc. ACM Special Interest Group on Computer Graphics and Interactive Techniques Conference, SIGGRAPH*, 2014.
[42] F. Weichert, D. Bachmann, B. Rudak, and D. Fisseler, "Analysis of the accuracy and robustness of the leap motion controller," *Sensors*, vol. 13, no. 5, pp. 6380–6393, 2013.
[43] D. C. Ruspini, K. Kolarov, and O. Khatib, "Haptic interaction in virtual environments," in *Proc. IEEE/RSJ International Conference on Intelligent Robots and Systems*, vol. 1, 1997, pp. 128–133.
[44] A. M. Lund, "Measuring usability with the use questionnaire12," 2001.
[45] A. Lecuyer, S. Coquillart, A. Kheddar, P. Richard, and P. Coiffet, "Pseudo-haptic feedback: can isometric input devices simulate force feedback?" in *Proc. IEEE Virtual Reality*, 2000, pp. 83–90.
[46] A. M. Genecov, A. A. Stanley, and A. M. Okamura, "Perception of a haptic jamming display: Just noticeable differences in stiffness and geometry," in *Proc. IEEE Haptics Symposium (HAPTICS)*, 2014, pp. 333–338.
[47] N. Gurari, K. J. Kuchenbecker, and A. M. Okamura, "Stiffness discrimination with visual and proprioceptive cues," in *Proc. World Haptics*, 2009, pp. 121–126.
[48] C. Pacchierotti, G. Salvietti, I. Hussain, L. Meli, and D. Prattichizzo, "The hring: a wearable haptic device to avoid occlusions in hand tracking," in *Proc. IEEE Haptics Symposium (HAPTICS)*, 2016, pp. 134–139.
[49] I. Hussain, G. Spagnoletti, C. Pacchierotti, and D. Prattichizzo, "A wearable haptic ring for the control of extra robotic fingers," in *Proc. Asia Haptics*, 2016.
[50] M. Maisto, C. Pacchierotti, F. Chinello, G. Salvietti, A. De Luca, and D. Prattichizzo, "Evaluation of wearable haptic systems for the fingers in augmented reality applications," *IEEE Transactions on Haptics*, 2017.

Francesco Chinello received the M.S. degree in Computer Engineering (focus on Robotics and Industrial automation) in 2010 from the University of Siena with a thesis entitled "System software for rapid prototyping of anthropomorphic manipulators." On February 2014, he received his Ph.D. on Information Engineering. After that, he has been Post-Doc at the SIRSLab (University of Siena) and a guest researcher at the Department of Advanced Robotics (Italian Institute of Technology). Since January 2017, he is an Assistant Professor of the Department of Business Development and Technology, Aarhus School of Business and Social Science, at Herning (Denmark).

Claudio Pacchierotti (S'12, M'15) received the Ph.D. degree from the University of Siena, Italy, in 2014. He has been a postdoctoral researcher at the Dept. of Advanced Robotics of the Italian Institute of Technology, Genova, Italy in 2015 and 2016. He visited the University of Padua, University of Pennsylvania, and University of Twente in 2013, 2014, and 2015, respectively. He received the 2014 EuroHaptics Best PhD Thesis Award for the best doctoral thesis in the field of haptics, and the 2015 Meritorious Service Award for his work as a Reviewer for the IEEE Transactions on Haptics. He has also been Associate Editor for the 2017 IEEE World Haptics conference as well as the Publicity Chair for the 2017 IEEE World Haptics and 2018 Asia Haptics conferences. He is currently a CR2 researcher of the CNRS at Irisa and Inria Rennes Bretagne Atlantique, France, in the Lagadic group. His research deals with robotics and haptics, focusing on cutaneous feedback techniques, wearable devices, shared control, and haptics for robotic surgery.

Monica Malvezzi (M'12) has been Assistant Professor of Mechanics and Mechanism Theory at the Dept. of Information Engineering and Mathematics of the University of Siena since 2009. She has been visiting scientist at Istituto Italiano di Tecnologia, IIT, in Genova, Italy, since 2015. She received the Laurea degree in Mechanical Engineering from the University of Florence in 1999 and the Ph.D. degree in Applied Mechanics from the University of Bologna in 2003. From 2002 to 2008 she was researcher at the University of Florence, Energy Department. Her main research interests are in control of mechanical and mechatronic systems, robotics, haptics, vehicle localization, multibody dynamics, grasping and dexterous manipulation.

Domenico Prattichizzo (F'15) received the Ph.D. degree in Robotics and Automation from the University of Pisa in 1995. Since 2002 he is an Associate Professor of Robotics at the University of Siena and since 2009 he is a Scientific Consultant at Istituto Italiano di Tecnoloogia. In 1994, he was a Visiting Scientist at the MIT AI Lab. Since 2014, he is Associate Editor of Frontiers of Biomedical Robotics. From 2007 to 2013 he has been Associate Editor in Chief of the IEEE Transactions on Haptics. From 2003 to 2007, he has been Associate Editor of the IEEE Transactions on Robotics and IEEE Transactions on Control Systems Technologies. He has been Chair of the Italian Chapter of the IEEE RAS (2006-2010), awarded with the IEEE 2009 Chapter of the Year Award. Research interests are in haptics, grasping, visual servoing, mobile robotics and geometric control. He is currently the Coordinator of the IP collaborative project "WEARable HAPtics for Humans and Robots" (WEARHAP).